PHYSICAL REVIEW B **95**, 161109(R) (2017)

Quantum spin Hall density wave insulator of correlated fermions

Gaurav Kumar Gupta and Tanmoy Das
Department of Physics, Indian Institute of Science, Bangalore 560012, India
(Received 30 July 2016; revised manuscript received 19 January 2017; published 17 April 2017)

We present the theory of a new type of topological quantum order which is driven by the spin-orbit density wave order parameter, and distinguished by a Z_2 topological invariant. We show that when two oppositely polarized chiral bands [resulting from the Rashba-type spin-orbit coupling α_k; k is crystal momentum] are significantly nested by a special wave vector $\mathbf{Q} \sim (\pi,0)/(0,\pi)$, it induces a spatially modulated inversion of the chirality ($\alpha_{k+Q} = \alpha_k^*$) between different sublattices. The resulting quantum order parameters break translational symmetry, but preserve time-reversal symmetry. It is inherently associated with a Z_2-topological invariant along each density wave propagation direction. Hence it gives a weak topological insulator in two dimensions, with even number of spin-polarized boundary states. This phase is analogous to the quantum spin Hall state, except here the time-reversal polarization is spatially modulated, and thus it is dubbed quantum spin Hall density wave (QSHDW) state. This order parameter can be realized or engineered in quantum wires, or quasi-two-dimensional systems, by tuning the spin-orbit coupling strength and chemical potential to achieve the special nesting condition.

DOI: 10.1103/PhysRevB.95.161109

Introduction. A topological state of matter can arise when two bands with opposite chirality are inverted across the Fermi level at odd number of time-reversal invariant momenta (TRIM) [1–3]. One of the prerequisites is thus to obtain a momentum dependence of the spin state or chirality, which is often triggered by the spin-orbit coupling (SOC). The inversion of the chirality between the bulk conduction and valence bands across the insulating band gap at the TRIM is protected by the time-reversal (TR) symmetry, leading to a Z_2 topological insulator (TI). At the boundary, both chiral states meet at the TRIM with gapless edge or surface states. Within the Dirac Hamiltonian notation, the inverted bulk band gap (denoted by $m < 0$) at the TRIM provides the negative Dirac mass, while the associated gapless boundary states produce Dirac cones.

While strong quantum fluctuations or disorder are often detrimental to the band topology, they can conversely drive the inversion of the chiral bands with nontrivial topological properties. These states are not always defined by a Landau order parameter, but rather distinguished by a topological invariant of the correlated electronic bands. Examples of such states include topological Mott [4,5], Kondo [6], and Anderson [7] insulators. The antiferromagnetic order parameter can give a distinct topological class which breaks time-reversal and translation symmetries, but preserves their combinations [5]. To date, TIs have been realized in various noninteracting systems including HgTe/CdTe [8,9], InAs/GaSb [10] quantum wells for two-dimensional (2D) TIs, and Bi-based chalcogenides for three-dimensional TIs [11–15]. SmB_6 [6,16] and YbB_6 [17] have been extensively studied both theoretically and experimentally as potential candidates for topological Kondo insulators.

Proposal. We develop the theory of a Landau-type topological order parameter driven by staggered chiral band inversion. The order parameter arises from the translational symmetry breaking due to Fermi-surface (FS) nesting between Rashba-type SOC (RSOC) split bands. Such nesting between opposite chiral states may occur in 2D systems or quantum wires of Bi, Pb, Sb, and similar elements in which both SOC and interaction are large [18,19]. The nesting strength is enhanced with reduced system dimensionality and thickness [18,19]. Our theory relies on a particular nesting vector $\mathbf{Q} \sim (\pi,0)$ or $(0,\pi)$, where the helicity of the RSOC $\alpha_{\mathbf{k}} = \alpha_R(\sin k_y - i \sin k_x)$ (with α_R being the RSOC strength and k_x,k_y are the crystal momenta) is reversed to $\alpha_{\mathbf{k}+\mathbf{Q}} = \alpha_{\mathbf{k}}^*$. This is the key feature responsible for modulated chiral band inversion. We find that as a Landau-type order parameter develops due to this FS instability, it leads to a negative Dirac mass and insulating band gap. Along the direction of the nesting, we find that correlated electronic bands are associated with a nontrivial Z_2 invariant, with spin-polarized zero-energy boundary states. Such a state can be compared with a noninteracting quantum spin Hall (QSH) insulator in 2D, with the distinction that here every alternative atom possesses opposite chirality in the same valence band, owing to translational symmetry breaking, as illustrated in Fig. 1(b). Thus we call it a quantum spin Hall density wave (QSHDW) insulator.

Theory of QSHDW. To develop the theory of QSHDW, we use a single band tight-binding model in a 2D lattice with RSOC. The FS nesting is generally known to increase as the dimensionality is reduced. For this reason, we use anisotropic tight-binding hoppings along the x and y directions (t_x and t_y), so that the nesting at the wave vector $Q = (\pi,0)$ or $(0,\pi)$ can be monitored by changing the ratio t_x/t_y. The concept and formalism of the QSHDW is general for any dimension as long as the corresponding nesting wave vector allows for the chirality inversion at all given dimensions. We use a tight-binding dispersion with nearest-neighbor hopping as $\xi_{\mathbf{k}} = -2[t_x\cos(k_x a) + t_y\cos(k_y b)] - \xi_F$, where ξ_F is the chemical potential, and a and b are the lattice constants along the x and y directions, respectively. For the RSOC $\alpha_{\mathbf{k}}$ we assume an isotropic SOC strength, α_R for simplicity.

The noninteracting dispersion with RSOC is shown in Fig. 2(a), with two horizontal arrows dictating the $\mathbf{Q}$ nesting vectors connecting the two helical bands. For our numerical calculations, we use $t_y/t_x = 0.2$, $\xi_F = 0$, and $\alpha_R = -1.25/t_x$, which are realistic parameters for Bi-surface state grown on Ag thin films [20]. For Bi and Pb atomic wires with one monolayer coverage, the intrinsic value of the FS nesting is $\sim(0.42\pi/a,0)$ [18,20]. Starting from this band parameter, we estimate that

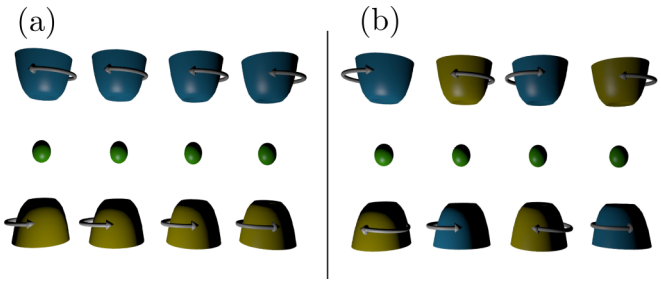

FIG. 1. Distinction between a QSH and QSHDW insulator in real space. (a) A typical QSH insulator where all lattice sites have the same chirality in the valence band. (b) The QSHDW insulator where two sublattice sites have the opposite chirality in the valence band.

the required chemical potential shift to obtain the $(\pi,0)$ nesting is about $1.74t_x$, which can be achieved with chemical doping or gating or varying thickness, among others.

The interaction term responsible for the emergence of the QSHDW can be sought from on-site Hubbard, or Hund's coupling or Heisenberg interaction, as shown explicitly in the Supplemental Material (SM) [21]. Here we use a generalized form as

$$H_{\rm int} = g \sum_{\substack{\mathbf{k}_1-\mathbf{k}_4,\\ \sigma_1-\sigma_4}} c^{\dagger}_{\mathbf{k}_1,\sigma_1} c_{\mathbf{k}_2,\sigma_2} c^{\dagger}_{\mathbf{k}_3,\sigma_3} c_{\mathbf{k}_4,\sigma_4}, \tag{1}$$

where g is the strength of the on-site interaction. $c^{\dagger}_{\mathbf{k},\sigma}$ ($c_{\mathbf{k},\sigma}$) is the creation (annihilation) operator for an electron with Bloch momentum $\mathbf{k}$, and spin $\sigma = \pm$.

We define a four-component Nambu-Gor'kov spinor $\Psi_{\mathbf{k}} = (c_{\mathbf{k},\uparrow}, c_{\mathbf{k},\downarrow}, c_{\mathbf{k}+\mathbf{Q},\uparrow}, c_{\mathbf{k}+\mathbf{Q},\downarrow})$. For the particular type of nesting depicted in Figs. 2(a) and 2(b), one singlet and two possible triplet order parameters can develop as

$$\text{Singlet:}\langle O_1\rangle = \sum_{\mathbf{k}} \langle \bar{\Psi}_{\mathbf{k}} | \Gamma_1 d_{1\mathbf{k}} | \Psi_{\mathbf{k}} \rangle, \tag{2}$$

$$\text{Triplet:}\langle O_2\rangle = \sum_{\mathbf{k}} \langle \bar{\Psi}_{\mathbf{k}} | \Gamma_2 d_{2\mathbf{k}} + \Gamma_3 d_{3\mathbf{k}} | \Psi_{\mathbf{k}} \rangle, \tag{3}$$

$$\langle O_3\rangle = \sum_{\mathbf{k}} \langle \bar{\Psi}_{\mathbf{k}} | \Gamma_4 d_{4\mathbf{k}} | \Psi_{\mathbf{k}} \rangle, \tag{4}$$

where the Dirac Γ matrices have the representation $\Gamma_{(1,2,3,4,5,6,7)} = (\tau_y\otimes\sigma_y, \tau_x\otimes\sigma_x, \tau_x\otimes\sigma_y, \tau_x\otimes\sigma_z, \tau_z\otimes\mathbb{I}, \tau_z\otimes\sigma_x, \tau_z\otimes\sigma_y)$ in the same spinor Ψ. τ_i and σ_i are the 2×2 Pauli matrices in the sublattice and spin basis, respectively, and $\mathbb{I}$ is the 2×2 identity matrix. Except for Γ_1 and Γ_5, all other Γ matrices here are odd under TR symmetry. Here, we are interested only in the TR invariant order parameters for Z_2 topological consequence. Therefore, the TR invariance of these order parameters requires that the structure factor $d_{i\mathbf{k}}$ must complement the symmetry of the corresponding Γ_i matrices under TR symmetry. Therefore $d_{1\mathbf{k}}$ for the singlet state must be even under TR symmetry, while all three $d_{2,3,4}$ for the triplet states must be odd under TR symmetry. In what follows, the order parameters can be either even parity and spin singlet or odd parity and spin triplet. This is also consistent with the fermionic antisymmetric property of the order parameters.

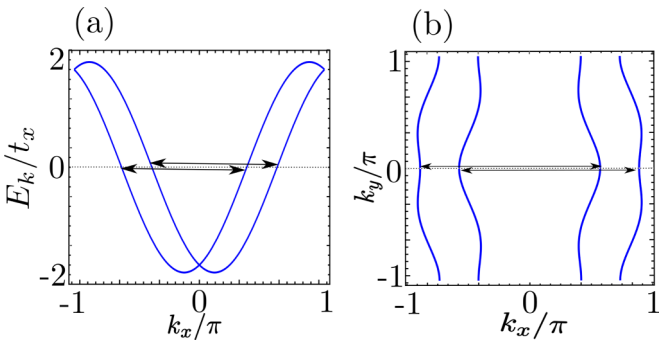

FIG. 2. FS topology. (a) Noninteracting RSOC split bands are plotted along k_x with $k_y = 0$. Black horizontal arrows show the nesting vectors. (b) We show the nesting on the quasi-1D FS.

These order parameters introduce electronic gap terms as $\Delta_i = g\langle O_i\rangle$. All order parameters govern the nontrivial topological phase as to be shown later. For the singlet case, we take $\Delta_{1\mathbf{k}} = \Delta_{10}$ (s wave) without losing generality. For the triplet gaps $\Delta_{2,3}$, we find through self-consistent solution (see Supplemental Material [21]) that Δ_2 has a higher probability to form and possesses a larger amplitude than the Δ_3 term. Henceforth, we thus consider only the Δ_2 term for the triplet case. We consider a p-wave form factor for the odd-parity term as $\Delta_{2\mathbf{k}} = \Delta_{20}\sin(k_x a)$. We note that the essential topological character deduced here does not depend on the form factor, which will be clearer below. At $\mathbf{Q} = (\pi,0)$ or $(0,\pi)$, the mean-field Hamiltonian can be fully expressed in terms of the Dirac matrices as (for singlet)

$$H_1(\mathbf{k}) = \xi^{+}_{\mathbf{k}} I_{4\times 4} + \xi^{-}_{\mathbf{k}}\Gamma_5 + \alpha'_{\mathbf{k}}\Gamma_6 + \alpha''_{\mathbf{k}}\Gamma_7 + \Delta_{10}\Gamma_1, \tag{5}$$

and eigenvalues:

$$E_{1k} = \xi^{+}_{k} \pm \sqrt{(\xi^{-}_{k} \pm |\alpha_k|)^2 + \Delta^2_{10}}, \tag{6}$$

and for triplet:

$$H_2(\mathbf{k}) = \xi^{+}_{\mathbf{k}} I_{4\times 4} + \xi^{-}_{\mathbf{k}}\Gamma_5 + \alpha'_{\mathbf{k}}\Gamma_6 + \alpha''_{\mathbf{k}}\Gamma_7 + \Delta_{2\mathbf{k}}\Gamma_2, \tag{7}$$

and eigenvalues:

$$E_{2k} = \xi^{+}_{k} \pm |\alpha_k| \pm \sqrt{(\xi^{-}_{k})^2 + \Delta^2_{2,\mathbf{k}}}. \tag{8}$$

Here $\xi^{\pm}_{\mathbf{k}} = (\xi_{\mathbf{k}} \pm \xi_{\mathbf{k}+\mathbf{Q}})/2$, and $\alpha'_{\mathbf{k}}$ and $\alpha''_{\mathbf{k}}$ are the real and imaginary parts of the RSOC (α_k). In analogy with the Dirac Hamiltonian, we can easily recognize that $\xi^{-}_{\mathbf{k}}$ gives the Dirac mass term which controls the topological phase transition, while $\Delta_{\mathbf{k}}$ helps open an electronic gap between the opposite chiral states.

A few remarks are in order about why the present mean-field model gives correct results in such quasi-1D systems. In quasi-1D systems, one may expect that a Luttinger-liquid theory might be more appropriate. However, experimentally it is demonstrated that at finite temperature and in the presence of impurity scattering, the quantitative difference between the Luttinger-liquid and Fermi-liquid behavior is small and often undetectable [22]. Therefore, a Fermi-liquid-like physics with mean-field order parameter can be used here. Moreover, in the weak-coupling region, quantum fluctuations are Fermi-liquid like, i.e., it scales quadratically with energy. Such weak fluctuations only become appreciable near the quantum critical regime where the gap becomes small. Away from the

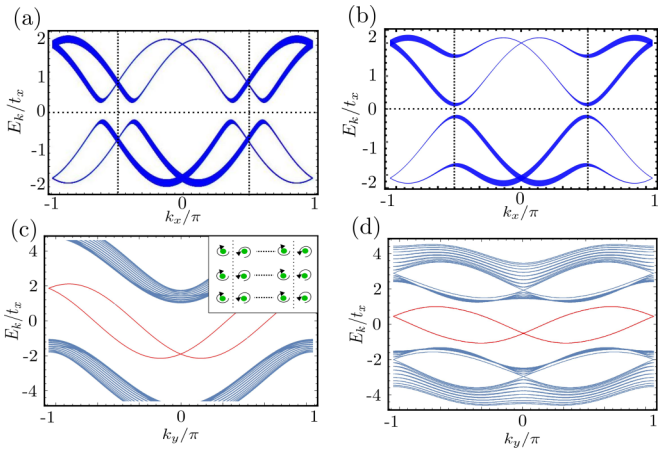

FIG. 3. Electronic dispersion and edge states in quasi-1D strip geometries. (a),(b) We plot the electronic band structure at $k_y = 0$ for singlet and triplet states, respectively. The width of each line dictates the corresponding electronic weight in the QSHDW state. The vertical dashed lines give the RBZ boundaries. (c),(d) Edge states in quasi-1D strip geometries for the singlet and triplet state, respectively. We show the spectrum of the interacting quasi-1D QSHDW in a strip geometry (inset).

critical region, the QSHDW order is robust against quantum fluctuations.

Electronic insulator. For a pure 1D case ($t_y/t_x \to 0$), any infinitesimally small value of Δ produces an insulating band gap. As the FS warping increases with increasing t_y/t_x, some parts of the FS (which are not nested by $\mathbf{Q}$) remain ungapped for small values of Δ (topological invariant may still be defined for the cases with small FS pockets, giving rise to QSHDW semimetals). With larger Δ, an insulating gap appears. The critical value of Δ required for the insulating state increases with increasing t_y/t_x.

In Figs. 3(a) and 3(b), we demonstrate the electronic dispersion for a QSHDW triplet (singlet) insulator. The vertical width of each line in Figs. 3(a) and 3(b) dictates the electronic weight associated with the main bands [thickness of the line corresponds to the contribution from the first reduced Brillouin zone (RBZ)]. As the main and shadow bands possess different spin-orbit chirality (due to $\alpha_{k+Q} = \alpha_k^*$), the emergence of QSHDW order is naturally accompanied by chirality inversion at the time-reversal symmetric momenta. In the present QSHDW theory, due to noncollinearity of the spin coming from the SOC, the spin expectation value of two different bands at each sublattice cancel each other, and thus the system preserves TR symmetry.

Topological properties. For the calculation of topological invariants in a single-particle picture (also applicable to mean-field electronic bands), Kane and Mele proposed the concept of "TR polarization." This is a Z_2 analog of the charge polarization for an integer quantum Hall state [23,24]. TR polarization depends on the number of times an electron exchanges its "TR partner" between its Bloch state, $\psi_n(\mathbf{k})$, and its TR conjugate $\psi_m^\dagger(-\mathbf{k})$ in half of the BZ. This is essentially quantified by the Pfaffian of a matrix with components $w_{mn}(\mathbf{k}) = \langle\psi_m(-\mathbf{k})|T|\psi_n(\mathbf{k})\rangle$, where $T = i\mathbb{I}\otimes\sigma_y K$ (K is the complex conjugate operator) is the TR operator, and n and m are valence-band indices. The relative sign of $\mathrm{Pf}[w(k)]$ between any two TR invariant k points becomes opposite if the electron switches its TR partner an odd number of times in traversing between them. This, in other words, implies that $\mathrm{Pf}[w(k)]$ vanishes at an odd number of momenta in between the two high-symmetric k points [23]. The Z_2 invariant ν is defined as

$$\nu = \frac{1}{2\pi i}\int_L d\mathbf{k}\cdot\nabla_{\mathbf{k}}\log[P(\mathbf{k}) + i\delta], \tag{9}$$

where L covers half the BZ. As $P(\mathbf{k}_i^*) = 0$, the residue theory dictates that $\nu = 1$. If there are odd number of $P(k) = 0$, one obtains $\nu = 1$ (modulo 2), otherwise, $\nu = 0$. According to the Kane-Mele criterion, there are three Z_2 invariants in 2D: (ν_0:$\nu_1\nu_2$), where ν_0 is the net Z_2 invariant giving a strong topological insulator, while $\nu_{1,2}$ are the weak topological invariants representing an odd number of band inversions along the x and y directions, respectively.

In the present 1D case, the chirality or the TR polarizibility is reversed along the direction of the nesting. For both singlet and triplet cases, we find that $\mathrm{Pf}[w]$ changes sign when going from $k_x = 0$ to $k_x = \pi$, and it vanishes at $k_x = \pi/2$, but not in the perpendicular directions. Therefore, the system possesses a strong Z_2 topological invariant ($\nu_1 = 1$) along this direction (in 1D), but a weak topological insulator in 2D with invariants (0:10). This behavior also makes our model distinct from the Kane-Mele model of the QSH insulator in graphene which is defined by Z_2 invariant (1:00).

Boundary state. Due to the bulk boundary correspondence, the nontrivial Z_2 invariant implies the existence of zero-energy edge states as long as the TR symmetry is held. The present system resembles a Su-Schrieffer-Heeger [25] -type model in 1D if we map the two atoms with opposite chirality in a larger unit cell as two sublattices. Therefore, the topological invariant in the bulk dictates a single end state inside the gap. The end state is localized at the two ends of the lattice in the nesting direction (here x direction), but disperses along the y direction. They are further split by the RSOC.

To show the behavior of these edge states, we investigate a strip geometry [see *inset* to Fig. 3(d)] with open boundary condition along the x direction while keeping the periodic boundary condition along the y direction. Splitting the corresponding Hamiltonian into three parts as $H_{\mathrm{strip}} = H_1 + H_2 + H_{12}$, where H_1 and H_2 are the noninteracting terms in the first and second RBZ, while H_{12} is the interaction term, we get

$$H_1 = \sum_{k_y,j,\sigma}{}' \Big[-2t_y\cos(k_y)c^\dagger_{k_y,j,\sigma}c_{k_y,j,\sigma} - t_x c^\dagger_{k_y,j,\sigma}c_{k_y,j\pm1,\sigma} + \alpha_R\sin(k_y)c^\dagger_{k_y,j,\sigma}c_{k_y,j,\bar\sigma} - \lambda\frac{\alpha_R}{2}c^\dagger_{k_y,j,\sigma}c_{k_y,j+\lambda,\bar\sigma}\Big], \tag{10}$$

$$H_{12}^s = \Delta_{10}\sum_{k_y,j.\sigma}{}' [e^{iQ_x j}c^\dagger_{k_y,j,\sigma}c_{k_y,j,\bar\sigma} + e^{-iQ_x j}c^\dagger_{k_y,j,\sigma}c_{k_y,j,\bar\sigma}], \tag{11}$$

$$H_{12}^t = -i\Delta_{20}/2\sum_{k_y,j,\sigma}{}' [e^{-iQ_x(j+1)}c^\dagger_{k_y,j,\sigma}c_{k_y,j+1,\bar\sigma} - e^{-iQ_x(j-1)}c^\dagger_{k_y,j,\sigma}c_{k_y,j-1,\bar\sigma} + \mathrm{H.c.}]. \tag{12}$$

Here $H_2 = H_1(\mathbf{k} \to \mathbf{k} + \mathbf{Q})$. The index $\lambda = \pm 1$ takes care of the fact that for the RSOC, the nearest-neighbor (spin-flip) hopping along the $\pm\mathbf{r}$ directions have opposite sign. j is the lattice site index along the x direction, and the prime on the summation indicates that it is restricted within the corresponding RBZ. $H_{12}^{t/s}$ corresponds to the triplet/singlet case. Also, the first c in $H_{12}^{t/s}$ belongs to the k sublattice while the second c belongs to the $(k + Q)$ sublattice. The eigenvalues of H_{strip} are plotted in Fig. 3 with $\Delta_0 = 1.48t_x$ $(3.3t_x)$ for triplet (singlet). This gap value requires an interaction strength of $g \approx 3.3t_x$ $(5.0t_x)$. It should be noted that the interaction strength chosen to show the edge state is much higher than the value required to open the insulating gap. For each 1D strip, the $\nu_1 = 1$ invariant dictates zero-energy end states (Zak phase). The nearest-neighbor end states are coupled to each other by RSOC, and thus are split at all k_y values except at the TR invariant points. Since the bulk system is a weak topological insulator, the boundary states are not immune to perturbations, as also evident from the presence of an even number of Dirac nodes in the BZ.

2D extension. Finally, we explore a 2D system in which we explicitly include both nestings $Q_x = (\pi,0)$ and $Q_y = (0,\pi)$, which makes the Hamiltonian in Eqs. (5) and (7) a 6×6 one. In such case, the topological properties become difficult to deduce analytically. Numerically, we find that Pf$[w]$ changes sign every time while going from one TRIM point to another, in both the x and y directions, giving rise to the weak Z_2 invariant (0:11), a 2D QSHDW insulator.

Conclusions. We presented the theory of a new state of matter, called QSHDW state, which is a spontaneous symmetry breaking quantum phase associated with a nontrivial Z_2 invariant. The design and synthesis of quasi-2D atomic quantum wires have become a routine laboratory exercise, and it has been extensively shown that both intrinsic and extrinsic tunings of electronic properties, SOC, and Coulomb interaction are very easy in such geometry [19]. In fact, the FS nesting between different helical states is observed in a number of quasi-1D [18] and 2D systems [26]. Moreover, it is shown that the FS nesting properties, RSOC, as well as the charge screening process can be monitored by varying sample thickness and substrate [18,26]. In this connection, ferroelectric or polar substrates can also have a versatile role in enhancing SOC and interaction strength.

1D SOC is recently observed in an optical lattice, where our idea can also be explored with the existing setups. From a theoretical perspective, the generalization of the proposed topological phase to higher dimensional FS with the same nesting condition along all directions is possible. For example, noncentrosymmetric heavy-fermion materials would be potential candidates to explore a large SOC interaction. Therefore, we envision that the emergence of a QSHDW insulator may open a new area in the field of interaction-induced TIs.

Acknowledgments. The work is facilitated by the computer cluster facility at the Department of Physics at the Indian Institute of Science. We acknowledge funding from the Department of Science and Technology (DST), India under Young Research Scientist Award given through the SERB.

[1] A. Bansil, H. Lin, and T. Das, Rev. Mod. Phys. **88**, 021004 (2016).
[2] X.-L. Qi and S.-C. Zhang, Rev. Mod. Phys. **83**, 1057 (2011).
[3] M. Z. Hasan and C. L. Kane, Rev. Mod. Phys. **82**, 3045 (2010).
[4] S. Raghu, X.-L. Qi, C. Honerkamp, and S.-C. Zhang, Phys. Rev. Lett. **100**, 156401 (2008).
[5] R. S. K. Mong, A. M. Essin, and J. E. Moore, Phys. Rev. B **81**, 245209 (2010).
[6] M. Dzero, K. Sun, V. Galitski, and P. Coleman, Phys. Rev. Lett. **104**, 106408 (2010).
[7] J. Li, R.-L. Chu, J. K. Jain, and S.-Q. Shen, Phys. Rev. Lett. **102**, 136806 (2009).
[8] B. A. Bernevig, T. L. Hughes, and S.-C. Zhang, Science **314**, 1757 (2006).
[9] M. König, S. Wiedmann, C. Brüne, A. Roth, H. Buhmann, L. W. Molenkamp, X.-L. Qi, and S.-C. Zhang, Science **318**, 766 (2007).
[10] I. Knez, R.-R. Du, and G. Sullivan, Phys. Rev. Lett. **107**, 136603 (2011).
[11] J. C. Y. Teo, L. Fu, and C. L. Kane, Phys. Rev. B **78**, 045426 (2008).
[12] D. Hsieh, D. Qian, L. Wray, Y. Xia, Y. S. Hor, R. Cava, and M. Z. Hasan, Nature (London) **452**, 970 (2008).
[13] H. Zhang, C.-X. Liu, X.-L. Qi, X. Dai, Z. Fang, and S.-C. Zhang, Nat. Phys. **5**, 438 (2009).
[14] Y. Xia, D. Qian, D. Hsieh, L. Wray, A. Pal, H. Lin, A. Bansil, D. Grauer, Y. Hor, R. Cava *et al.*, Nat. Phys. **5**, 398 (2009)
[15] Y. Chen, J. Analytis, J.-H. Chu, Z. Liu, S.-K. Mo, X.-L. Qi, H. Zhang, D. Lu, X. Dai, Z. Fang *et al.*, Science **325**, 178 (2009).
[16] M. Dzero, J. Xia, V. Galitski, and P. Coleman, Annu. Rev. Condens. Matter Phys. **7**, 249 (2016).
[17] T.-R. Chang, T. Das, P.-J. Chen, M. Neupane, S.-Y. Xu, M. Z. Hasan, H. Lin, H.-T. Jeng, and A. Bansil, Phys. Rev. B **91**, 155151 (2015).
[18] C. Tegenkamp, D. Lükermann, H. Pfnür, B. Slomski, G. Landolt, and J. H. Dil, Phys. Rev. Lett. **109**, 266401 (2012).
[19] C. Brand, H. Pfnür, G. Landolt, S. Muff, J. Dil, T. Das, and C. Tegenkamp, Nat. Commun. **6**, 8118 (2015).
[20] T. Das, Phys. Rev. Lett. **109**, 246406 (2012).
[21] See Supplemental Material at http://link.aps.org/supplemental/10.1103/PhysRevB.95.161109 for the details of the calculations.
[22] D.-W. Wang, A. J. Millis, and S. Das Sarma, Phys. Rev. Lett. **85**, 4570 (2000).
[23] C. L. Kane and E. J. Mele, Phys. Rev. Lett. **95**, 146802 (2005).
[24] L. Fu and C. L. Kane, Phys. Rev. B **76**, 045302 (2007).
[25] W. P. Su, J. R. Schrieffer, and A. J. Heeger, Phys. Rev. Lett. **42**, 1698 (1979).
[26] H. Bentmann, S. Abdelouahed, M. Mulazzi, J. Henk, and F. Reinert, Phys. Rev. Lett. **108**, 196801 (2012).